Geophys. J. Int. (2009) **176,** 601–613 doi: 10.1111/j.1365-246X.2008.03995.x

Modelling temporal variation of surface creep on the Chihshang fault in eastern Taiwan with velocity-strengthening friction

Shu-Hao Chang,[1] Wei-Hau Wang[2] and Jian-Cheng Lee[3]

[1] *Institute of Seismology, National Chung Cheng University, Taiwan*
[2] *Institute of Applied Geophysics, National Chung Cheng University, Taiwan. E-mail: seiwhwg@eq.ccu.edu.tw*
[3] *Institute of Earth Sciences, Academia Sinica, Taiwan*

Accepted 2008 September 30. Received 2008 August 5; in original form 2007 March 2

SUMMARY

The active Chihshang fault at the boundary between the Eurasian and the Philippine Sea plates along the Longitudinal Valley in eastern Taiwan is creeping near the surface but has also produced large earthquakes at mid-crustal depth such as the 2003, M_w 6.5, Chengkung earthquake. The creep rate measured at the surface shows strong seasonal fluctuations before the Chengkung earthquake, correlated with groundwater pressure variations measured at nearby wells. The Chengkung earthquake did not rupture the fault near the surface but induced a sudden increase of creep rate that decayed with time during the postseismic period. These observations suggest that the near surface fault obeys a rate-strengthening friction law. We conduct numerical simulations based upon the observed variations of creep rate with regard to a velocity-strengthening friction law and 1-D groundwater diffusion model to investigate the fault rheology behind this phenomenon. The model, which assumes a creeping fault segment extending from the surface to a depth of 5 km, yields a good fit to the creep data when the friction parameters are assumed to vary with depth or to have changed at the time of the Chengkung earthquake. Our best model suggests that the creeping zone is characterized by a rate parameter $a = \partial\mu/\partial\log(V)$ of 1.3×10^{-2} and a friction coefficient of 0.84, and a long-term slip rate of 25.9 mm yr^{-1} at depths less than 87 m. By contrast, the lower segment of the creeping zone exhibits a much lower friction coefficient of 0.19, a smaller a of 6.6×10^{-3} and a higher long-term slip rate of 38.1 mm yr^{-1} at depths between 0.087 and 5.0 km. This change in rate parameters implies that the lithologies or physical properties of the fault rocks may vary with depth. Alternatively, a model assuming a dramatic increase in rate parameter from 5.6×10^{-4} to 6.2×10^{-3} by the strong ground shaking of the Chengkung earthquake can also yield a fair agreement with the observed data. The lack of a notable deceleration in fault creep rate during the dry period from 2002 to mid-2003 suggests that the real recharging system for the fault zone may be more complicated than what we assumed in this study.

Key words: Friction; Fault zone rheology.

1 INTRODUCTION

Aseismic creep is an intriguing phenomenon observed in many fault zones and is usually associated with poorly consolidated material, high pore pressure or elevated temperature (Scholz 2002). Fault creep is often observed following stress perturbations. For example, postseismic creep is believed to be a consequence of stress transfer from the rupture of asperities onto surrounding velocity-strengthening fault patches (Marone *et al*. 1991; Hearn *et al*. 2002; Miyazaki *et al*. 2004; Perfettini & Avouac 2004; Pollitz 2005; Hsu *et al.* 2006). This implies that a measure of fault creep can serve as a gauge of stress if the frictional parameters are known, or conversely, if both creep rates and stress perturbations are known, then frictional parameters can be derived.

In this paper, we apply this later approach to examine the Chihshang fault, a 35-km-long reverse fault within the Longitudinal Valley of eastern Taiwan (Fig. 1). The 150-km-long, NNE-trending Longitudinal Valley marks the suture zone between the Eurasian and the Philippine Sea plates. Geodetic measurements from the last two decades indicate that the Chihshang fault has been undergoing rapid creep at an average rate of about 20–30 mm yr^{-1} (Yu & Liu 1989; Lee *et al*. 2003). It appears that aseismic creep dominates at depths shallower than 5 km because seismicity dramatically drops above that depth and the rupture of the 2003 $M_w = 6.5$ Chengkung earthquake also terminated at this shallow level (Wu *et al*. 2006). In addition, the fault creep rate exhibits annual variations probably due to seasonal fluctuations in precipitation (Lee *et al*. 2003), analogous to what was observed at Parkfield, California and on the

© 2008 The Authors
Journal compilation © 2008 RAS

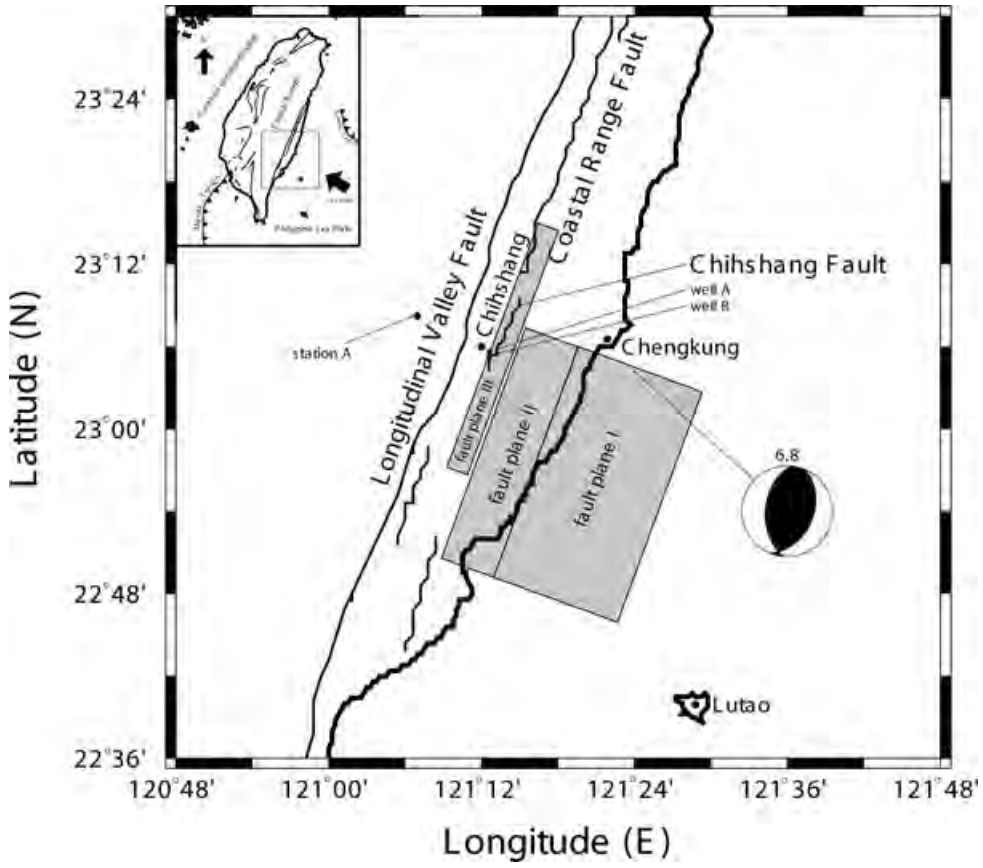

Figure 1. Geological setting of the Chihshang fault which separates the Philippine Sea plate to the east and the Eurasian plate to the west. Two monitoring water wells, indicated as solid triangles, have been recording water levels on a monthly basis since 1980. Rainfall records are collected at station A about 4 km away from the Chihshang fault. A set of creep meters operated by the Institute of Earth Sciences, Academia Sinica records horizontal creep motions of the fault daily. The 2003 Chengkung, Taiwan earthquake ($M_w = 6.8$) caused a major slip along the Chihshang fault with a thrust focal mechanism, as determined by the Broadband Array in Taiwan for Seismology (BATS). The areas marked with Faults 1 and 2 are the vertical projections of the two fault patches ruptured during 2003 Chengkung earthquake (Wu *et al.* 2006); Fault 3 is the map view of the creep zone of the Chihshang fault suggested in this study.

Hayward fault (Lienkaemper *et al*. 2001; Roeloffs 2001). Also, following the Chengkung earthquake, the creep rate dramatically increased up to about five times that in its preseismic period (Lee *et al*. 2005, 2006).

In this study, we test whether the creeping zone of the Chihshang fault obeys a velocity-strengthening friction law and to what extent the changes in water level are responsible for the episodic motion. We also attempt to explore whether the creeping zone is frictionally homogeneous. Answering these questions would shed light on the mechanics of creep along the Chihshang fault and earthquake hazards in this area.

2 SEISMOTECTONIC SETTING

GPS measurements indicate that the convergence rate between the Eurasian and the Philippine Sea plates in Taiwan is about 8.2 cm yr^{-1} on an azimuth of 310°, and that about one-third of it is taken up across the Longitudinal Valley (Yu *et al*. 1997). The 35-km-long Chihshang fault is a southern segment of the Longitudinal Valley fault zone. It separates the Lichi mélange, composed of exotic ophiolite and sedimentary blocks embedded in a sheared scaly argillaceous matrix in the hangingwall and the Quaternary alluvial deposits in the footwall. The aftershocks outline a well-defined listric fault geometry (Chen & Rau 2003; Lin 2004; Lee *et al*. 2006). The dip of the Chihshang fault is about 60°–80° near the Earth's surface and gradually decreases to 20°–30° at depths of 20–25 km. Furthermore, at shallow levels, an anticlinal folding has been developing in the hangingwall near the fault trace (Lee *et al*. 2006).

3 DATA

3.1 Creep meter data

In this study, we use the 1999–2004 creep meter data, recorded on daily basis and published previously (Lee *et al*. 2003, 2005). We use the sum of the horizontal shortening on three creep meters along three parallel branches of the Chihshang fault at the Chinyuan site (Lee *et al*. 2003, Fig. 2) to derive the net slip on the Chihshang fault based on its attitude and the rake of fault slip given by Lee *et al*. (2003). Combining field observations and local geodetic network measurements, Lee *et al*. (2006) indicated that the three branches, within a 120-m-wide deformation zone, probably all splay from a single primary fault plane. Surface horizontal shortening is accommodated by these three branches of fractures which implies that the creep meters data indeed represent most of slip on the primary fault plane of the Chihshang fault at the surface level. The data show that (1) before the Chengkung earthquake, the Chihshang fault was horizontally shortening at a rate of about 15 mm yr^{-1} on average with strong annual fluctuations; (2) at the surface, the fault did not slip during the Chengkung earthquake and (3) the creeping rate

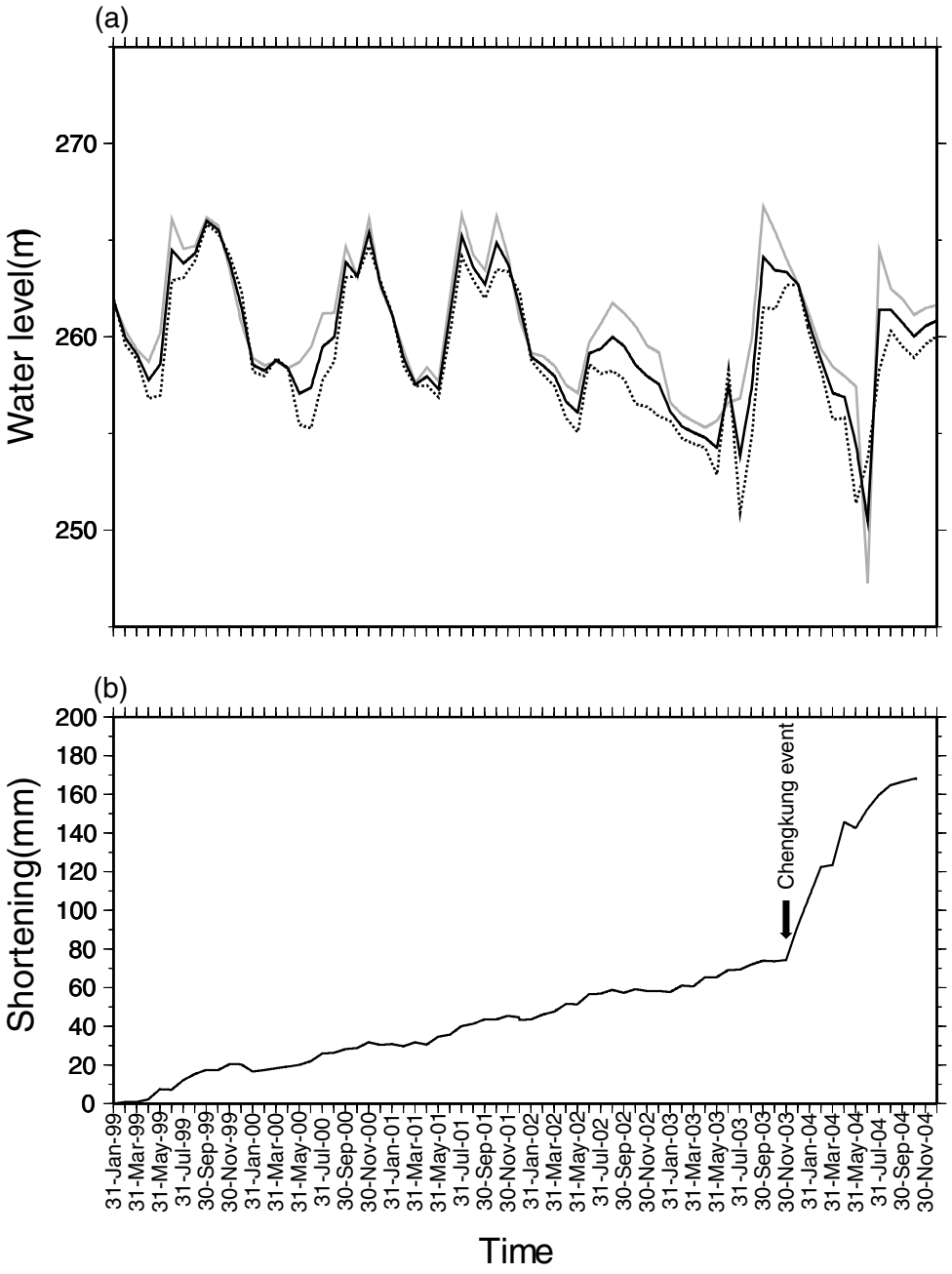

Figure 2. (a) Temporal variations in water levels. The grey line represents the water level above sea level as measured in well A; the dashed line represents the water level measured in well B and the black line depicts the average water level measured in wells A and B (data from the Water Resource Agency, Ministry of Economic Affairs, Taiwan). (b) Cumulative horizontal shortening measurements across the Chihshang fault from 1999 to 2004.

increased suddenly at the time of the earthquakes and then decayed thereafter (Fig. 2).

3.2 Groundwater level and rainfall

We collected groundwater level data measured by the Water Resource Agency at two wells located at Chinyuan and Fuhsing near the creep meters running across the Chihshang fault zone (Fig. 1). Fig. 2 illustrates the fluctuations of water levels measured in these two wells and the corresponding horizontal shortening observed by the creep meters. It is clear that both wells share a similar trend of temporal variations in water levels but the mean value of the water level measured in well B is few metres higher than that measured in well A. The well-screen depth for both wells was set up to be about 50 m below Earth's surface and 30 m below the mean underground water level. Contemporary precipitation was recorded by the Central Weather Bureau at station A, which is about 4 km away from the Chihshang fault as shown in Fig. 1. Fig. 3 shows the temporal variations in groundwater levels and the contemporary precipitation as well as the de-trended fault creep data. It clearly shows a strong correlation among the groundwater, the precipitation and the fault creep, especially before the 2003 Chengkung earthquake. It is also noteworthy that the temporal variations in average groundwater levels of the two wells show an approximately 50-d phase

© 2008 The Authors, *GJI*, **176,** 601–613
Journal compilation © 2008 RAS

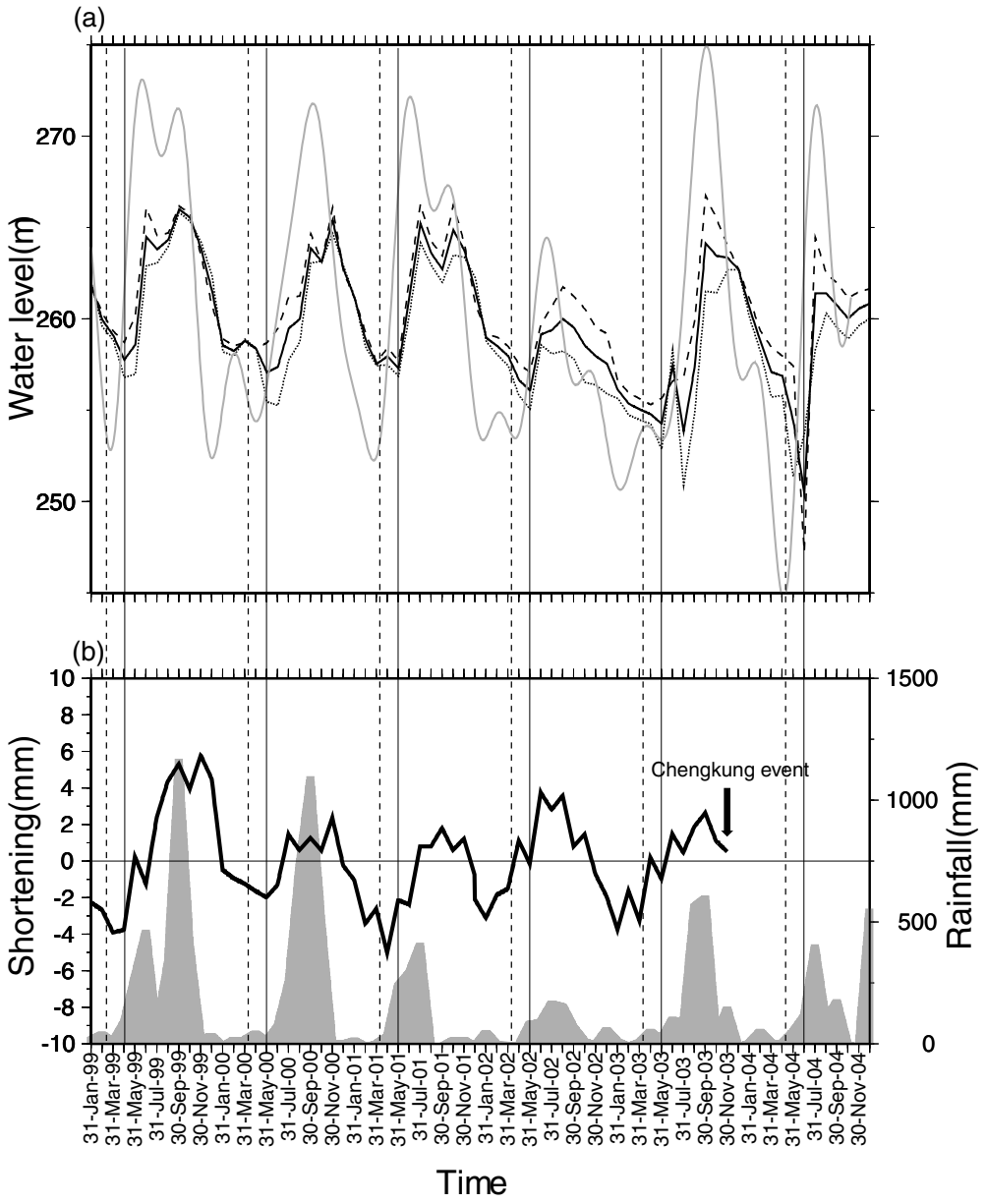

Figure 3. (a) Temporal variations in the average underground water level (black line) and the estimated water table (grey line). The dashed and dotted curves represent the water levels measured at Wells A and B, respectively. (b) De-trended horizontal shortening measurements across the Chihshang fault from 1999 to the day before the Chengkung earthquake (solid curve). The grey shaded areas depict daily rainfall. Note that the times of the monitored rising water table (the solid time lines) are about 50 d later than the times of the increased rainfall (dashed time lines).

lag compared to the variations in precipitation, estimated from our cross-correlation analysis.

If infiltration through the vadose zone is much faster than the baseflow from the water table to the well-screen depth, the phase lag can be used to estimate near-surface hydraulic diffusivity by employing an analysis of 1-D half-space diffusion due to periodic fluctuation of water table (Todd 1959). Theoretically, a given periodic fluctuation of water table, $\Delta P_{\max} \cos \omega t$, would result in the pore pressure variation in a half-space, such that

$$\Delta P(y,t) = \Delta P_{\max} \exp\left(-y\sqrt{\frac{\omega}{2\kappa}}\right) \cos\left(wt - y\sqrt{\frac{\omega}{2\kappa}}\right), \qquad (1)$$

where y is depth below mean water table; t is time; $\Delta P_{\max}$ is the amplitude of the periodic fluctuation in water pressure; ω is angular frequency and κ is hydraulic diffusivity. We thus obtain the corresponding phase lag Δt at depth y below mean water table

$$\Delta t = \frac{y}{\sqrt{2\kappa\omega}}. \qquad (2)$$

In the case of the two groundwater wells near the Chihshang fault, the annual variation of the water table, $\omega = 1.99 \times 10^{-7}$ rad s^{-1}, the screen depth to mean water table is 30 m, and the phase lag is 50 d. As a consequence, we obtain a hydraulic diffusivity of about 1.2×10^{-4} m^2 s^{-1} near the creep meter sites around the Chihshang fault. This value is about 3–4 orders of magnitude smaller than that measured in the near-surface gravel deposits at depths shallower than 30 m based upon a recent slug test (Dong *et al.* 2008). Our previous assumption of having a much more rapid infiltration rate

© 2008 The Authors, *GJI*, **176,** 601–613
Journal compilation © 2008 RAS

in the vadose zone is therefore valid. We will discuss this issue in more detail later.

With the derived hydraulic diffusivity and the fluctuation of pore pressure at the 30-m-deep screen depth $\Delta P(30, t)$, which can be expressed by a Fourier series, we are able to determine the fluctuation of pore pressure at depth of mean water table $\Delta P(0, t)$ by removing this diffusion effect based on eq. (1). Here, we define $\Delta P = \rho_w g \Delta h$, where ρ_w is density for water; g is gravitational acceleration and Δh is the deviation of water level from its mean value. We also employed a low-pass filter with a cut-off frequency of 0.009 d^{-1} to reduce high-frequency noise. As a result, we obtained an estimated water table, which had no time lag between it and the rainfall series (Fig. 3a).

3.3 Rupture model of the 2003 Chengkung earthquake

To estimate stress perturbations on the Chihshang fault plane caused by the 2003 Chengkung earthquake, we adopt the rupture source derived from accelometric records by Wu *et al*. (2006). The fault geometry is represented by a N20°E striking, two-segment fault with a 60°-dipping upper segment at depths of 5–18 km and a 45°-dipping lower segment at depths of 18–35.7 km (Fig. 1). The fault slip of Wu *et al.*'s model on the upper segment is 26 cm with a rake of 47.3°. On the lower segment, the yielded coseismic slip is 61.6 cm with a rake of 81.7°.

4 THEORY AND METHOD

We follow Perfettini & Avouac (2007) by assuming that the frictional behaviour of the creeping segment of the Chihshang fault obeys a pure velocity-strengthening rheology:

$$\tau = \sigma \mu_* + a\sigma \ln\left(\frac{V}{V_*}\right), \quad a > 0, \tag{3}$$

where τ and σ are the shear and effective normal stresses on the fault plane; μ_* is the friction coefficient under reference slip rate V_*; a is an empirical constant and V is fault slip rate. This is a simplified form of rate-and-state friction rheology (Ruina 1983; Dieterich 1994), which is

$$\mu(V, \theta) = \mu_* + a_{RS} \ln\left[\frac{V(t)}{V_*}\right] + b_{RS} \ln\left[\frac{\theta(t)}{\theta_*}\right], \tag{4}$$

where $\theta(t)$ and θ_* are state variables at time t and reference state, respectively; a_{RS} and b_{RS} are empirical constants. Perfettini & Avouac (2007) demonstrated that, when $a = a_{RS} - b_{RS}$, both rate-and-state and pure velocity-strengthening rheologies will lead to a similar fault slip subjected to relaxation of the creep rate following a stress step except during a transient phase.

The state of stress on a fault plane evolves as the combination of initial stress, stress change due to creep and stress change due to earthquake. As a result, for a fault plane with n subfaults, stress balance on a subfault i at time t requires

$$\tau(i, t) = \tau_0(i) + \Delta\tau_{creep}(i, t) + \Delta\tau_{eq}(i) \quad \text{and} \tag{5}$$

$$\sigma(i, t) = \sigma_0(i) + \Delta\sigma_{creep}(i, t) + \Delta\sigma_{eq}(i) - \Delta P_f(i, t), \tag{6}$$

where $\tau_0(i)$ and $\sigma_0(i) - \Delta P_f(i, t = 0)$ are the initial shear and effective normal stresses; $\Delta\tau_{creep}(i, t)$ and $\Delta\sigma_{creep}(i, t)$ are changes in shear and effective normal stresses by evolution of fault slip in the creeping zone; $\Delta\tau_{eq}(i)$ and $\Delta\sigma_{eq}(i)$ are shear and effective normal stresses induced by earthquakes; $\Delta P_f(i, t)$ is pore pressure change in the fault zone due to fluctuation of groundwater level.

In this study, we assume $\sigma_0(i) = \rho g z(i)(1 - \lambda)$, where $\rho = 2570$ kg m^{-3} represents the average density of rocks in the shallow crust in Taiwan (Yen *et al*. 1990); $z(i)$ is the depth of the subfault i and λ is the pore pressure ratio, which is assumed to be zero above the mean water table and 0.4 beneath that depth (meaning pore pressure is assumed hydrostatic). The value of σ_0 assumed above is valid if the fault is highly permeable. We will discuss this more in detail in Section 6.

Neglecting dynamic stress, we can express stress changes due to slip evolution as

$$\Delta\tau_{creep}(i, t) = \sum_{j=1}^{n} K_s(i, j)[u(j, t) - V_0(i)t], \; i = 1, n, \tag{7}$$

$$\Delta\sigma_{creep}(i, t) = \sum_{j=1}^{n} [K_n(i, j) - K_m(i, j)\beta] \times [u(j, t) - V_0(i)t], \quad i = 1, n, \tag{8}$$

where β is the Skempton's coefficient defined as the ratio of pore pressure change to mean stress change; $u(j, t)$ is the cumulative displacement of subfault j at time t; V_0 is long-term loading velocity and K_s, K_n and K_m are the elastic kernels for the shear, normal and mean stress changes induced by a unit slip on the subfault j in a given rake direction. In this study, we calculate the elastic kernels by employing the analytical solution of Okada (1992) for dislocation in an elastic half-space with the Lamé parameters being 3×10^{10} Pa. This dislocation model is also applied to evaluate coseismic static stress transfer by the Chengkung earthquake.

Note that K_n is in fact vanishing in this study as we assume that the subfaults are coplanar in the next section. In addition, we ignore the possible but small pore pressure changes induced by slip evolution or coseismic deformation. This is because the creeping fault zone either cuts through or is in contact with alluvial gravels, which may have a small Skempton's coefficient due to their low compressibility. Moreover, both creep movements and coseismic deformation by the Chengkung earthquake induce much smaller mean stress changes compared to shear stress changes on the creeping fault zone. Therefore, the pore pressure changes induced by slip evolution or coseismic deformation have little effect on ΔCFF. The evidence of no notable coseismic change in water level supports this argument. As a result, $\Delta\sigma_{creep}(i, t)$ in eq. (8) is vanishing.

The spatiotemporal variations in pore pressure in the creeping fault zone can be estimated by employing eq. (1) with the corrected groundwater level changes given in Section 3.1. Note that here we assume the hydraulic diffusivity of the fault zone, κ_f, is homogeneous and does not vary with time.

Combining eqs. (3), (5) and (6) and replacing V_* with V_0, we obtain that

$$V(i, t) = V_0(i) \exp\left[\frac{\Delta CFF(i, t)}{a(i)\sigma(i, t)}\right], \tag{9}$$

where $V(i, t)$ is the slip rate of subfault i at time t, and $\Delta CFF(i, t) = \Delta\tau(i, t) - \mu_0(i)\Delta\sigma(i, t)$ is the Coulomb stress change with $\mu_0(i)$ denoting the friction coefficient at long-term loading velocity $V_0(i)$, $\Delta\tau(i, t)$ and $\Delta\sigma(i, t)$ denoting the changes in shear and effective normal stresses of subfault i at time t with respect to their initial values. We solve eq. (8) with an implicit finite-difference method, such that

$$u_j^{i+1} = u_j^i + \Delta t V_0 \exp\left(\frac{\Delta CFF_j^i}{a\sigma_j^i}\right), \tag{10}$$

© 2008 The Authors, *GJI*, **176,** 601–613
Journal compilation © 2008 RAS

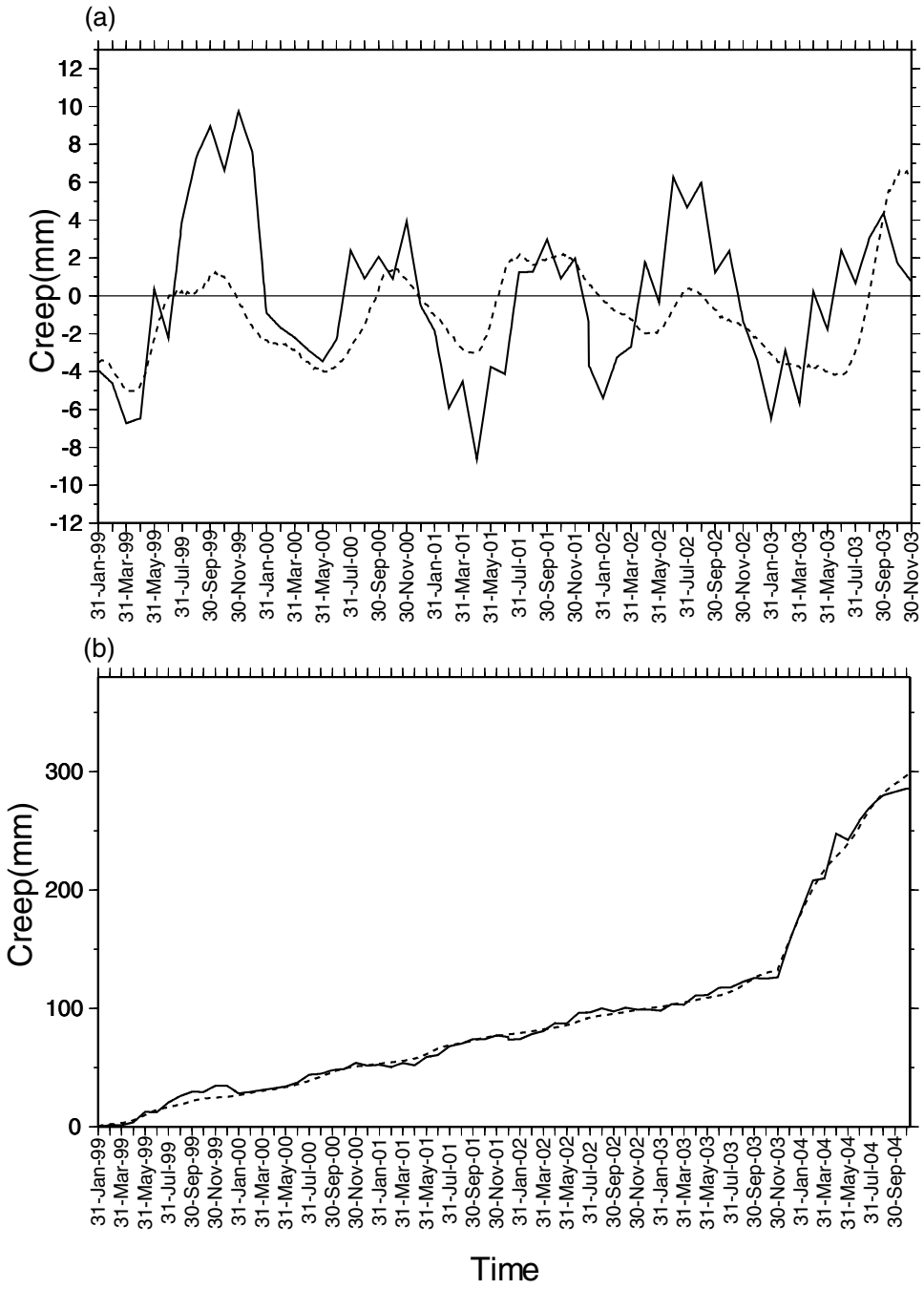

Figure 4. Simulated fault creep using a homogeneous rate-strengthening friction law model (Model A, Table 1) with frictional parameters inverted using creep measurements from 1999 to 2004. (a) Synthetic (dashed line) and observed (solid line) net creep from 1999 January to 2003 November after having de-trended steady creep. (b) Synthetic (dashed line) and observed net creep (solid line) from 1999 to 2004.

where u_j^i denotes the cumulative displacement at centre of the subfault j at time step i. The time interval Δt is restricted to be less than 1 d, and the corresponding slip is less than 1 mm to ensure a high resolution of our numerical analysis. Except for κ_f, which is resolved by grid searching in the range of $2 \times 10^{-5} - 6$ m^2 s^{-1}, the optimal values of a, μ_0 and V_0 are determined by employing the public genetic algorithm driver of Carroll (2004) to maximize an objective function (a goodness of fit criterion), which is defined as $r/\Delta s$, with r denoting the correlation coefficient between the observed and calculated creep series, and Δs denoting the root-mean-squared misfit between the observed and the modelled slip. We set up the searching range from 0.0005 to 0.02 for parameter a, from 0.1 to 0.85 for the friction coefficient μ_0 and from 1.0 to 100 mm yr^{-1} for the slip velocity V_0.

5 MODELS AND SIMULATION RESULTS

We employed a simplified fault plane oriented N20°E with a dip of 60°E to mimic the creeping zone of the Chihshang fault (Fig. 1). The model fault plane extends 35 km along the strike and 5.7 km along the dip. We further divided this fault plane into 143 subfaults

© 2008 The Authors, *GJI*, **176,** 601–613
Journal compilation © 2008 RAS

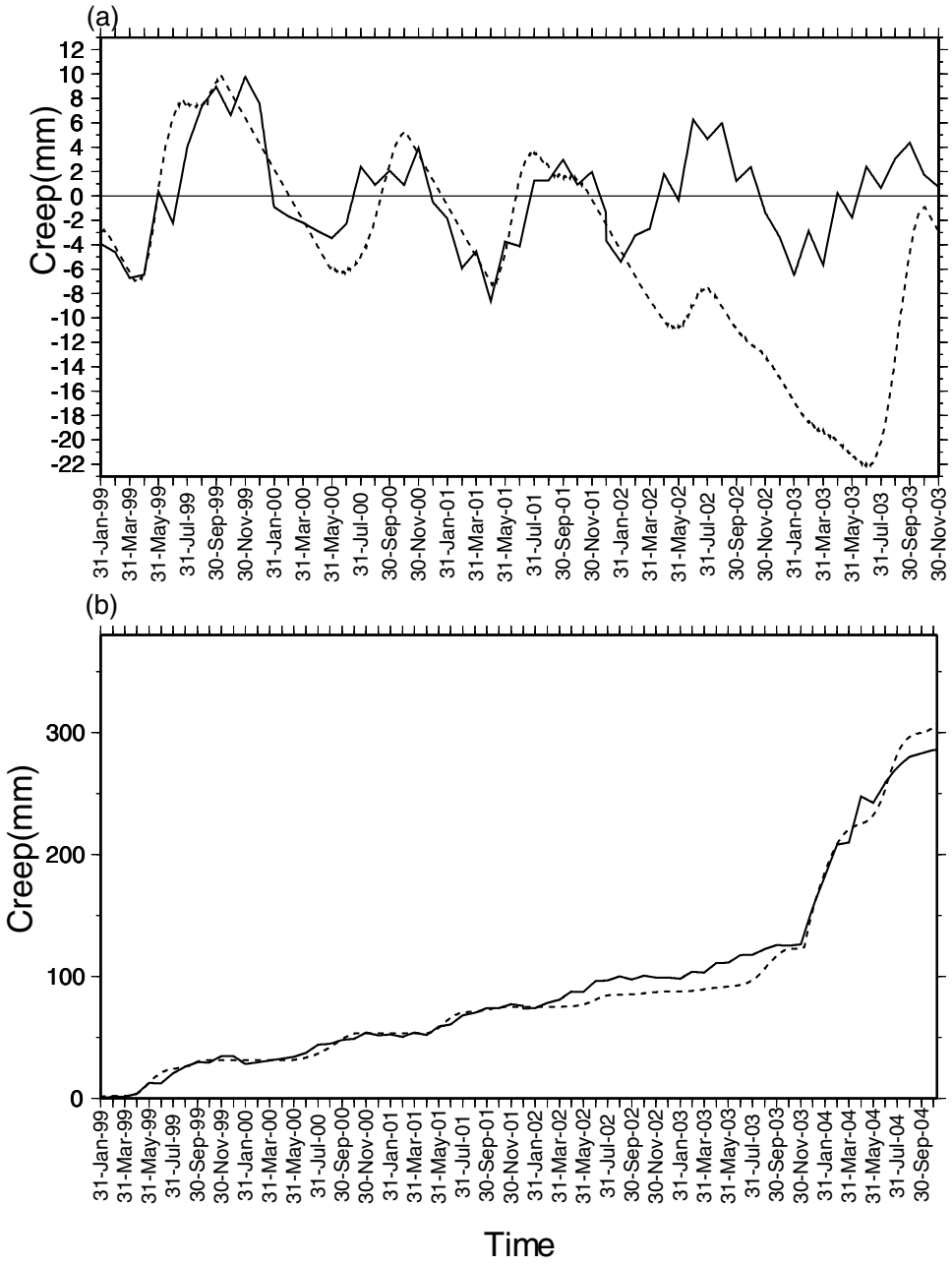

Figure 5. Fault creep modelled using a homogeneous rate-strengthening friction law model (Model B, Table 1) with inverted frictional parameters using creep measurements from 1999 to 2001. (a) Synthetic (dashed line) and observed (solid line) net creep from 1999 January to 2003 November after having de-trended steady creep. (b) Synthetic (dashed line) and observed (solid line) net creep from 1999 to 2004.

at different depths; each has a dimension of 35 km along the strike and 40 m along the dip. In our stress calculations, we adopted a uniform rake of 76°, as suggested by Lee *et al*. (2001).

While we assume that the creeping zone of the Chihshang fault is frictionally homogeneous, to fit the observed fault creep during the 1999–2004 period (Fig. 4), the optimal model (hereafter referred to as Model A) requires that the creeping zone has a friction coefficient μ_0 of 0.47, a rate parameter a of 7.0×10^{-3}, a hydraulic diffusivity κ_f of the creeping zone of 0 .50 $m^2\ s^{-1}$ and a long-term slip rate of 29.65 mm yr^{-1}. However, this model barely reproduces the episodic motions prior to the Chengkung earthquake (Fig. 4a). To improve the fit between the observations and the model predictions in the interseismic period, we first restrict the analysis to the interseismic creep data from 1999 to 2001 when annual rainfall was quite regular. It turns out that the episodic motion can be much better mimicked if a considerably higher μ_0 of 0.84, a smaller a of 2.6×10^{-3} and a slower V_0 of 24.43 mm yr^{-1} are employed (Fig. 5). However, in the trade-off, this model (hereafter referred to as Model B) fails to accurately predict fault creep during a subsequently relatively dry year (i.e. 2002); moreover, it produces a large misfit in the afterslip of the Chengkung earthquake.

In an attempt to improve model, we introduce spatial and temporal variations of friction and of long-term slip rate. We set up two models to evaluate the influence of fault heterogeneity. In Model C, we separated the creeping zone into two segments with a different μ_0 and a, and in Model D, additional change in V_0 for these two

© 2008 The Authors, *GJI*, **176,** 601–613
Journal compilation © 2008 RAS

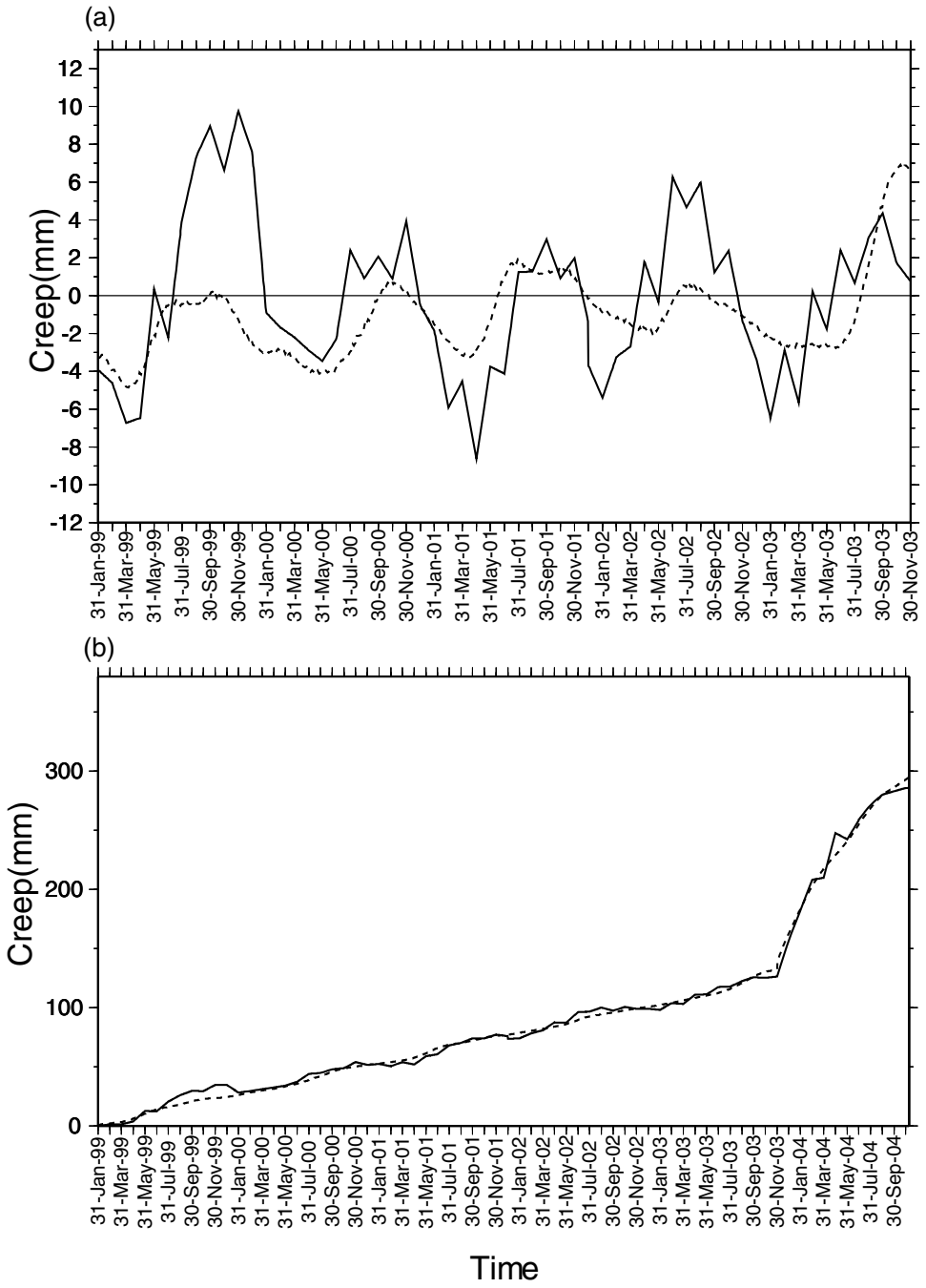

Figure 6. Simulated fault creep from a two-segment friction model (Model C, Table 1). Different values of μ_0 and a are applied to the upper and lower segments of the fault zone with frictional parameters inverted using creep measurements from 1999 to 2004. (a) Synthetic (dashed line) and observed (solid line) net creep from 1999 January to 2003 November after having de-trended steady creep. (b) Synthetic (dashed line) and observed (solid line) net creep from 1999 to 2004.

segments is taken into account. Estimates of parameter values in each fault segments and the bottom depth of the upper fault segment are simultaneously determined by best fitting the data based on a genetic algorithm. The results are shown in Figs 6 and 7 with optimal model parameters and goodness of fit listed in Table 1.

Alternatively, we constructed a model (Model E) that allows a to change after the Chengkung earthquake, implying that coseismic disturbance had altered the frictional behaviour of the fault zone. The result is shown in Fig. 8 with the optimal model parameters and fitness listed in Table 1.

6 DISCUSSION

Episodic creep has frequently been observed in geodetic studies (e.g. Gladwin *et al*. 1994; Lienkaemper *et al*. 2001), yet the driving mechanisms remain poorly understood. Several likely mechanisms have been proposed for such episodic motion, including the shrinking or swelling of soils due to changes in soil moisture and the oscillatory motion induced at the stability boundary (Du *et al*. 2003) or at a shallow velocity-weakening zone (Belardinelli 1997). There are also observations of seasonal variations such as snow loading

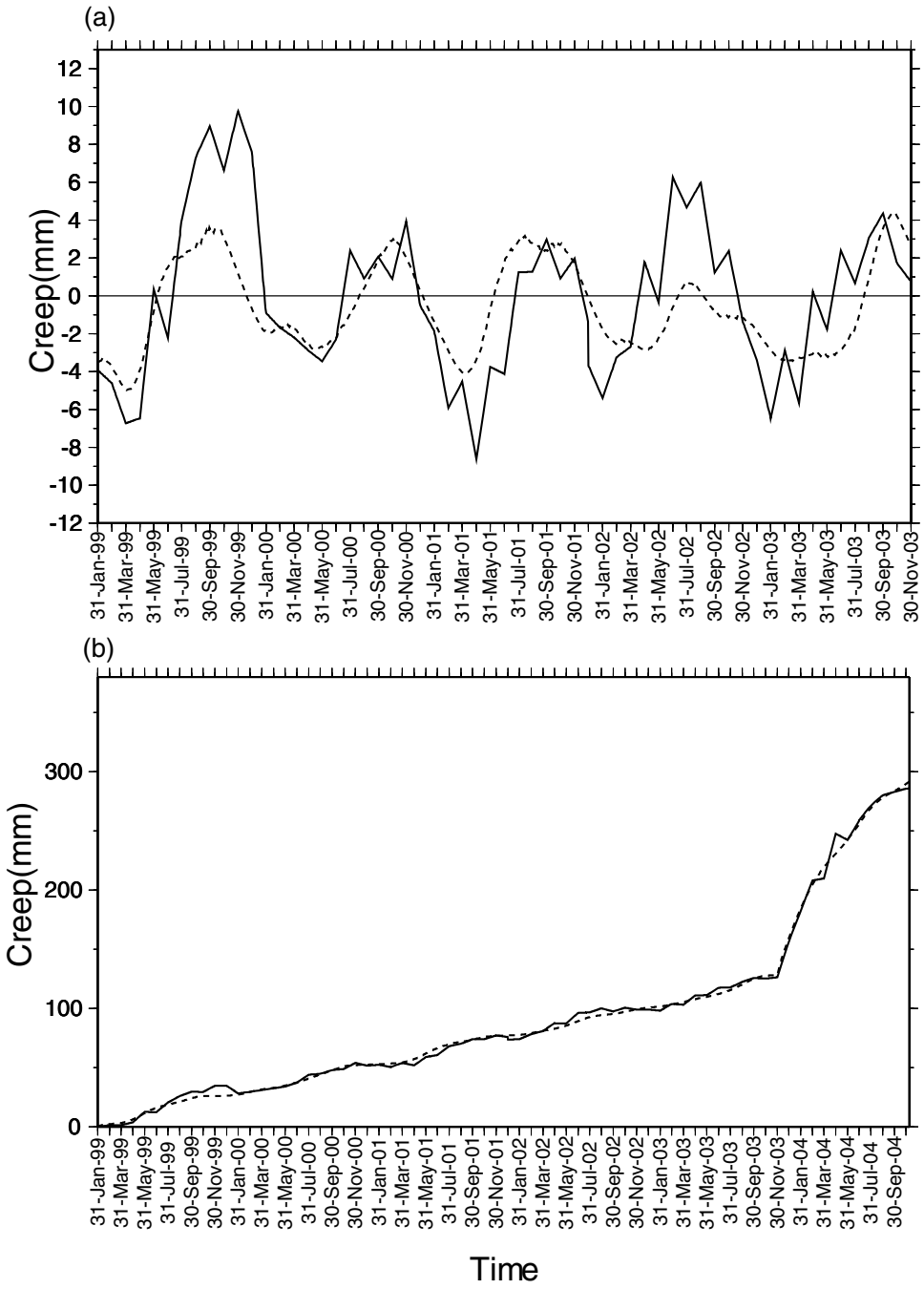

Figure 7. Simulated fault creep from a two-segment friction model (Model D, Table 1). Different values of μ_0, a and V_0 are applied to the upper and lower segments of the fault zone with frictional parameters inverted using creep measurements from 1999 to 2004. (a) Synthetic (dashed line) and observed (solid line) net creep from 1999 January to 2003 November after having de-trended steady creep. (b) Synthetic (dashed line) and observed (solid line) net creep from 1999 to 2004.

(e.g. Heki 2003) or land water storage (e.g. Bettinelli *et al.* 2008). As for the Chihshang fault, episodic creep events are apparently highly correlated with rainfall prior to the Chengkung earthquake. This observation agrees quite well with all our models in term of the occurrence time of the creep events despite the magnitudes of the modelled slips are somewhat underestimated. Model B apparently can best simulate the comparable episodic creep in 1999–2001 by adopting a larger hydraulic diffusivity $\kappa_f = 0.8\ \mathrm{m\,s^{-1}}$, a larger friction coefficient $\mu_0 = 0.84$ and a smaller rate parameter $a = 0.0026$. However, with these model parameters, Model B largely underestimates the amount of fault creep in the period during 2002 to mid-2003 when the average water level was much lower than that in the previous years (Fig. 2). The lack of distinct deceleration in creep rate observed in the dry period implies that it is impossible to accurately simulate the fault creep in regular and dry periods simultaneously. To accommodate this inconsistency, the other models, which consider the whole time-series tend to adopt a smaller hydraulic diffusivity, a smaller friction coefficient or a larger rate parameter to suppress the influence of fluctuations of water table as a trade-off. The lack of distinct deceleration in dry period may

© 2008 The Authors, *GJI*, **176,** 601–613
Journal compilation © 2008 RAS

Table 1. Model parameters and fitness.

	Hydraulic diffusivity ($m^2\ s^{-1}$)	a	Friction coefficient	V_0 (mm yr^{-1})	Bottom of upper fault segment (km)	Fitness (m^{-1})	rms misfit (mm)	Period considered
Model A	0.50	0.007	0.47	29.65		216.9	4.61	1999–2004
Model B	0.80	0.0026	0.84	24.43		359.1	2.78	1999–2001
Model C	0.80	0.0024[a] 0.007[b]	0.35[a] 0.39[b]	29.79	0.4	227.1	4.40	1999–2004
Model D	0.05	0.013[a] 0.0066[b]	0.84[a] 0.19[b]	25.93[a] 38.10[b]	0.087	296.1	3.38	1999–2004
Model E	0.08	0.00056[d] 0.0062[c]	0.45	26.84		263.9	3.79	1999–2004

[a]The upper fault segment.
[b]The lower fault segment.
[c]Before the Chengkung earthquake.
[d]After the Chengkung earthquake.

be caused by the uncertainty of the recharging system of the fault zone. We suspect that the water level within the fault zone in 2002 to mid-2003 might be underestimated based on the well records we employed, that is, the efficiency for water recharging to the fault zone and to the adjacent formations might be different. A more efficient water recharge to the fault zone is required to account for the notable increase in creep rate in the raining season during 2002 to mid-2003, when total precipitations and observed water table dropped significantly (Fig. 2). River recharge may be one possible way to make such an effect. Geological surveys show that the Chihshang fault is running across a river along the Longitudinal Valley. Because rivers can accumulate rainfall from overland flow, they might be able to recharge the fault zone more efficiently even in the relative dry period. However, water recharged from the river in the dry period is probably insufficient to significantly alter the water pressure in local aquifers because they are much thicker than the fault zone. Shrinkage of smectite-enriched soil, which is abundant in the Lichi mélange in the hangingwall (Liu *et al.* 1989), during the dry period could also enlarge the fracture openings in the fault zone and facilitated fast recharge to the fault zone. Nevertheless, these hypotheses still need to be tested by more sophisticated hydrogeological studies.

Because of the disagreement between observed water levels and fault slip in the dry period, our model parameters can vary in a broad range prior to the Chengkung earthquake or at shallow depth. For instance, rate parameter a can fall in a wide range of 5.6×10^{-4}–1.3×10^{-2} as employed in Models E and D. On the other hand, our models also indicate that the creeping fault must have a larger rate parameter $a \approx 7 \times 10^{-3}$ after the Chengkung earthquake or at deeper part of the fault to account for the afterslip (ref. Table 1).

Model D is our preferred model not only because it can best fit the observed data but also because it implies that the lower creeping segment has a higher long-term slip rate than the upper one, which is suitable for developing an anticline we observe. The high-friction and high velocity-strengthening materials in the uppermost 87 m inferred by this model may reflect loose gravel deposits at surface. Below it, the low-friction fault segment may be attributed to that the fault zone is in contact with the Lichi mélange, which has a very low friction angle of 12° (Fan 2002).

Model E is an alternative solution though the fitness is not as good as that of Model D. This model requires a dramatic increase in rate parameter at the time of the Chengkung earthquake. Large ground shaking has been reported to be able to loosen a seismogenic fault zone (Marone 2000). We suspect that the same mechanism might as well loosen a creeping fault. If so, the velocity-strengthening behaviour of the creeping fault could become more distinct by having loosened fault gouge. However, this scenario still needs to be justified by laboratory studies.

The rate parameter we obtained is comparable to many other studies worldwide. For example, the rate parameter $a \approx 6.6 \times 10^{-3}$–$1.3 \times 10^{-2}$ inferred from our best model is close to the value of 1.3×10^{-3}–10^{-2} derived from afterslip following the $M_w = 7.5$ Chi-Chi earthquake (Perfettini & Avouac 2004) and the measurements of 0.005–0.03 in laboratory experiments (Blanpied *et al.* 1995; Chester 1995). However, it is about an order of magnitude higher than those inferred from afterslip of the Peru earthquake (Perfettini *et al.* (2005)), the Nias-Simeulue earthquake (Hsu *et al.* 2006), the Parkfield earthquake (Johnson *et al.* 2006) and the Lander earthquake (Perfettini & Avouac 2007).

Our simulation results suggest the hydraulic diffusivity in the fault zone might be about 2–3 orders of magnitude larger than that in the footwall of the Chihshang fault. Such a large difference in hydraulic diffusivity has also been proposed for the San Andreas fault in Parkfield by Christiansen *et al.* (2007). The small vertical hydraulic diffusivity $\kappa \approx 1.2 \times 10^{-4}\ m^2\ s^{-1}$ estimated for the unconsolidated deposits on the footwall of the Chihshang fault is within the range of reported values for silt. A recent drilling project revealed that interbedded strata of slit and sandy gravel underlie a 30-m-thick layer of loose gravels in the hangingwall of the Chihshang fault (Dong *et al.* 2008). We suspect that the two observation wells employed in this study may have penetrated these interbedded strata, which leads to a small equivalent vertical hydraulic conductivity close to that of the confining layers due to layered heterogeneity (Leonards 1962). If so, the real temporal variations in water level might be smaller than what we inferred but larger than what observed in the two observation wells. However, without having the detailed logs of these two wells to indicate the thickness and the hydrogeological properties of the confining layers, we are not able to evaluate this influence precisely. Nevertheless, the difference between the real and the estimated water levels should be within a factor of 2.5, so is the rate parameter, since that is the maximum amplitude ratio between the estimated water table and the observed water levels (Fig. 2).

On the other hand, the larger hydraulic diffusivity of 0 .05–0 .8 $m^2\ s^{-1}$ we inferred for the fault zone, a typical value for gravels or fractured rocks, may result from slip-enhanced permeability by creating shear fractures or offsetting the confining layers. Fig. 9 shows the spatiotemporal variations in pore pressure changes respect to the pore pressure under mean water level with time and depth along the fault zone with $\kappa_f = 0.05\ m^2\ s^{-1}$ as suggested by

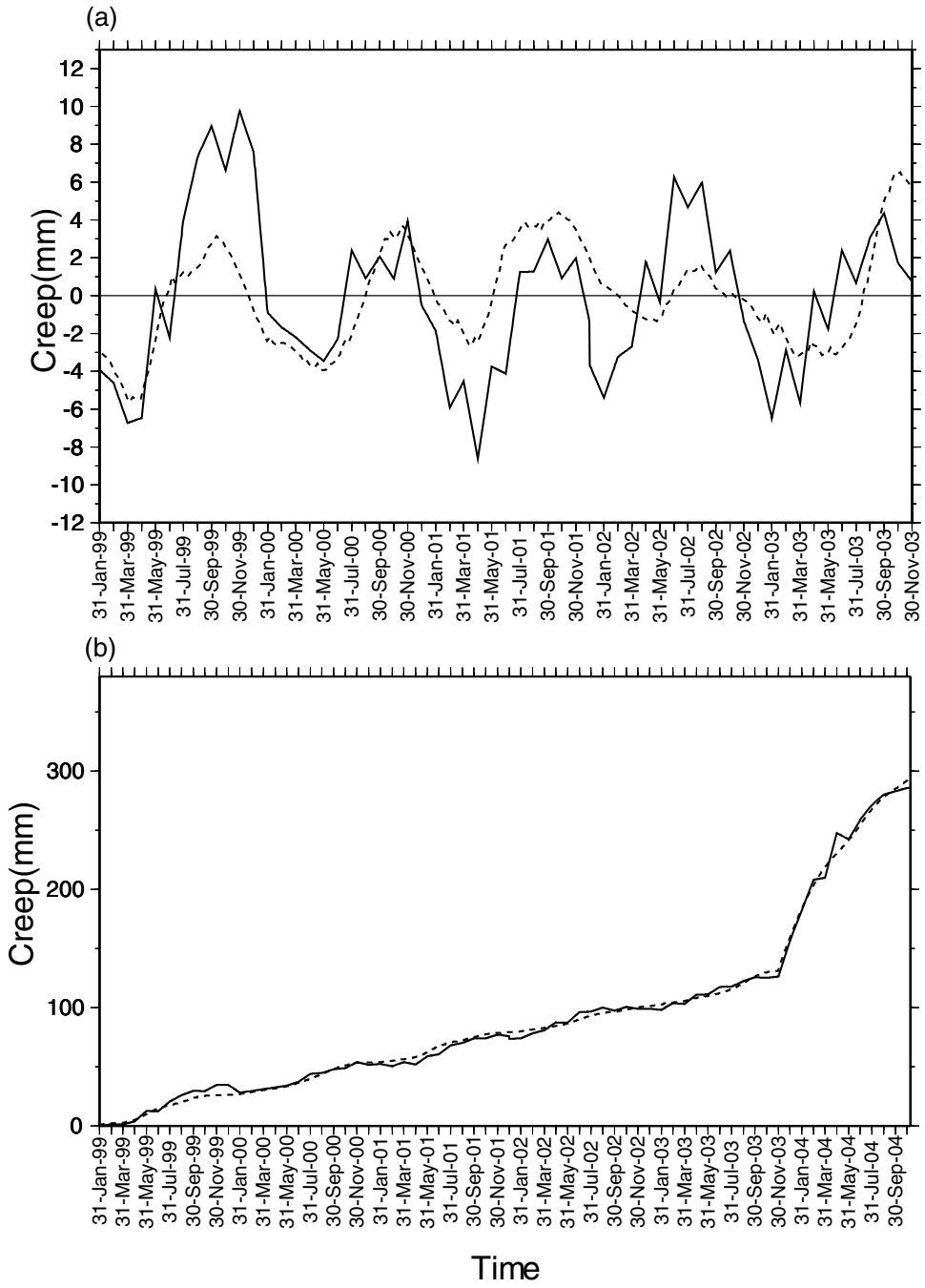

Figure 8. Simulated fault creep from Model E. Different values of a are applied to the fault zone before and after the Chengkung earthquake (Table 1). (a) Synthetic (dashed line) and observed (solid line) net creep from 1999 January to 2003 November after having de-trended steady creep. (b) Synthetic (dashed line) and observed (solid line) net creep from 1999 to 2004.

our best model. Note that the maximum depth for pore pressure to change by ± 0.2 bar is about 1.5 km. Such perturbations of pore pressure in high permeable fault zones are thought to be responsible for precipitation-induced earthquakes (Hainzl *et al.* 2006; Christiansen *et al.* 2007).

Chen & Rau (2003) pointed out that slip rate of the Chihshang fault varies from 22 mm yr^{-1} at depths of 12–15 km to 42–64 mm yr^{-1} at depths of 17–21 km by analysing 1487 repeating earthquakes along the Chihshang fault during 1991–2002. Their finding implies that prior to the Chengkung earthquake, the slip rate in the shallower seismogenic zone (12–15 km) is slower than that in the lower creeping segment (38.1 mm yr^{-1} at depths of 0.087–5 km) inferred from our best model and that in the deep seismogenic zone (17–21 km). This slip rate deficiency in the shallow seismogenic zone suggests that a large asperity was embedded there, which slowed down the slip rate until it broke and generated the Chengkung earthquake.

7 CONCLUSIONS

This study shows that creep rate variations on the Chihshang fault occur due to coseismic stress transfer or to seasonal variations of

© 2008 The Authors, *GJI*, **176,** 601–613
Journal compilation © 2008 RAS

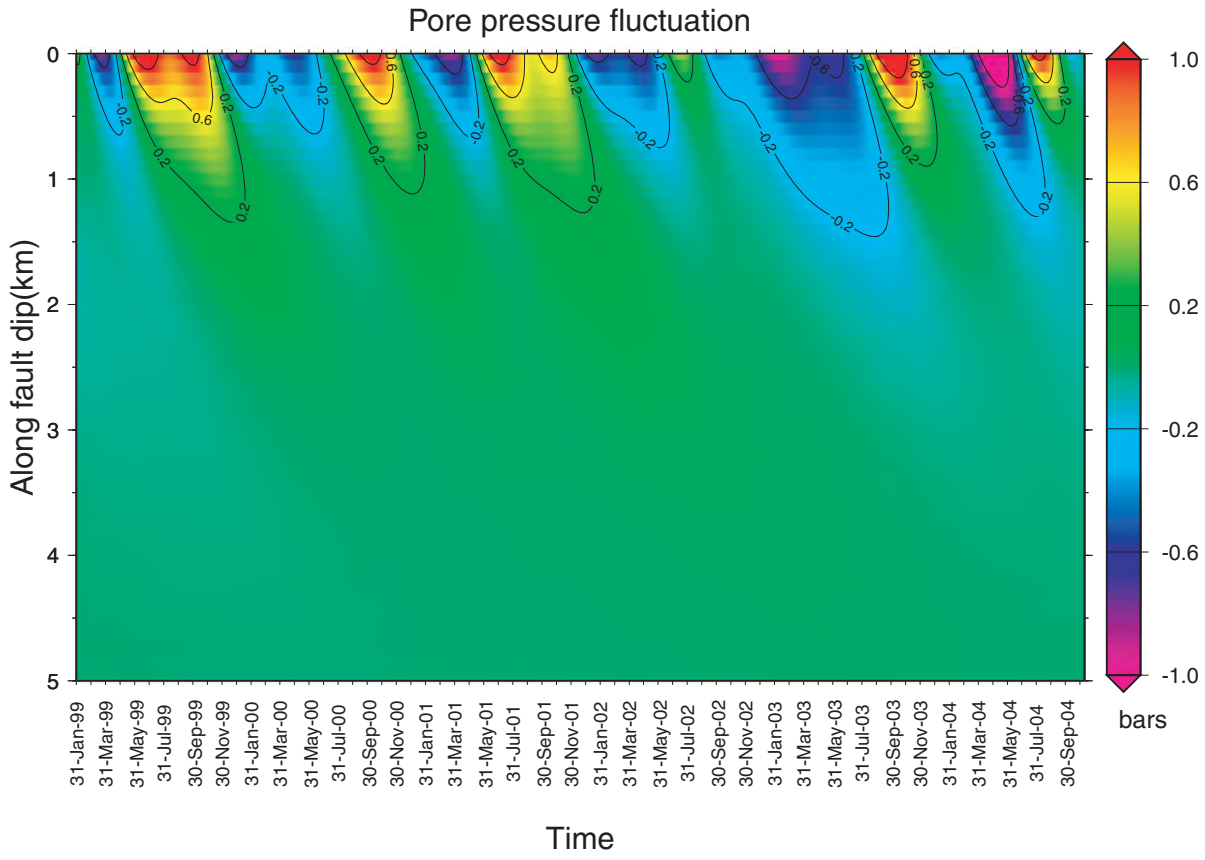

Figure 9. Spatiotemporal variations in pore pressure change in the fault zone during 1999–2004. The hydraulic diffusivity of the fault zone is assumed to be $0.05\,m^2\,s^{-1}$.

pore pressure, and that these variations can be explained reasonably well on the basis of a rate-strengthening friction law. We have demonstrated that the rheology of the Chihshang fault may vary at depth or to have changed at the time of the Chengkung earthquake to account for the observed variations of creep rate during 1999–2004. Our best model suggested that frictional parameters and long-term slip velocities change at depth of 87 m. Above that depth, the fault zone is characterized by having a large friction coefficient $\mu_0 = 0.84$ and high velocity-strengthening friction $a = 1.3 \times 10^{-2}$ but a smaller long-term slip rate $V_0 = 25.9$ mm yr^{-1}. Below that, a weak fault zone is required to have an extremely small friction coefficient $\mu_0 = 0.19$, a smaller rate parameter $a = 6.6 \times 10^{-3}$ and a higher long-term slip rate $V_0 = 38.1$ mm yr^{-1}. This model not only can best fit the observed creep data but also agrees well with geological observations. Alternatively, a scenario of a sudden increase in rate parameter from 5.6×10^{-4} to 6.2×10^{-3} at the time of the Chengkung earthquake can also yield a fair agreement with the observed data. In any cases, fault gouge with a rate parameter of about 7×10^{-3} at the deeper creeping fault zone or after the Chengkung earthquake is required to account for the afterslip following the Chengkung earthquake. The spatial or temporal change in rate parameter implies that either the lithologies or physical properties of the fault rocks vary with depth or the ground shaking at the time of the Chengkung earthquake was so strong that it loosened or altered the fault zone and enhanced the velocity-strengthening effect.

Although the creep rate of the Chihshang fault appears to be highly related to the fluctuations of the groundwater level, there is no notable deceleration in creep rate as we expect during the dry period of 2002 to mid-2003. This inconsistency suggests that the real recharging system for the fault zone may be more complicated than what we assumed in this study.

ACKNOWLEDGMENTS

We would like to thank the Water Resource Agency, Ministry of Economic Affairs, Taiwan, for providing us with water level data and the Central Weather Bureau for the precipitation data. We thank M. Cocos, J.-P. Avouac and M.E. Belardinelli for their valuable comments. This research was supported by the Taiwan Earthquake Research Center (TEC) funded through National Science Council (NSC) with grant numbers NSC 94-2116-M-194-004 and NSC 95-2475-M-194-001. The TEC contribution number for this article is 00042.

REFERENCES

Belardinelli, M.E., 1997. Increase of creep interevent intervals: a conceptual model, *Tectonophysics,* **277,** 99–107.

Bettinelli, P., Avouac, J.-P., Flouzat, M., Bollinger, L., Ramillien, G., Rajaure, S. & Sapkota, S., 2008. Seasonal variations of seismicity and geodetic strain in the Himalaya induced by surface hydrology, *Earth planet. Sci. Lett.,* **266,** 332–344.

Blanpied, M.L., Lockner, D.A. & Byerlee, J.D., 1995. Frictional slip of granite at hydrothermal conditions, *J. geophys. Res.,* **100,** 13 045–13 064.

Carroll, D.L., 2004. FORTRAN Genetic Algorithm (GA) Driver, available at http://cuaerospace.com/carroll/ga.html.

Chen, H.H., & Rau, R.J., 2003. Earthquake locations and style of faulting in an active arc-continent plate boundary: the Chihshang fault of eastern

Taiwan, *EOS, Trans. Am. geophys. Un.* (Fall Meet. Suppl., Abstract), **83,** T61B-1277.

Chester, F., 1995. A rheologic model for wet crust applied to strike-slip faults, *J. geophys. Res.,* **100,** 13 033–13 044.

Christiansen, L.B., Hurwitz, S. & Ingebritsen, S.E., 2007. Annual modulation of seismicity along the San Andreas Fault near Parkfield, CA, *Geophys. Res. Lett.,* **34,** doi:10.1029/2006GL038634.

Dieterich, J., 1994. A constitutive law for rate of earthquake production and its application to earthquake clustering, *J. geophys. Res.,* **99,** 2601–2618.

Dong, J.-J., Mu, C.-H., Lee, J.-C., Guglielmi, Y., Angelier, J. & Lin, C.-P., 2008. Structure geological model in the active Chihshang Fault zones: based on subsurface explorations and hydrogeological data in eastern Taiwan, in *Proceedings of Chinese Geological Annual Congress, May 7, 2008* Tainan, Taiwan.

Du, W.X., Sykes, L.R., Shaw, B.E. & Scholz, C.H., 2003. Triggered aseismic fault slip from nearby earthquakes, static or dynamic effect? *J. geophys. Res.,* **108,** doi:10.1029/2002JB002008.

Fan, C.F., 2002. Mechanical properties of Lichi talus in the Chihshang area, *M.S. thesis*. National Chung Hsing University, Taiwan, R.O.C.

Gladwin, M.T., Gwyther, R.L., Hart, R.H.G. & Breckenridge, K.S., 1994. Measurements of the strain field associated with episodic creep events on the San Andreas fault at San Juan Bautista, California, *J. geophys. Res.,* **99,** 4559–4565.

Hainzl, S., Kraft, T., Wasssermann, J., Igel, H. & Schmedes, E., 2006. Evidence for rainfall-triggered earthquake activity, *Geophys. Res. Lett.,* **33,** doi:10.1029/2006GL027642.

Hearn, E.H., Bürgmann, R. & Reilinger, R.E., 2002. Dynamics of Izmit earthquake postseismic deformation and loading of the Düzce earthquake hypocenter, *Bull. seism. Soc. Am.,* **92,** 172–193.

Heki, K., 2003. Snow load and seasonal variation of earthquake occurrence in Japan, *Earth planet. Sci. Lett.,* **207,** 159–164.

Hsu, Y.J. *et al*., 2006. Frictional afterslip following the 2005 Nias-Simeulue earthquake, Sumatra, *Science,* **312,** 1921–1926.

Johnson, K., Fielding, E.J., Rolandone, F. & Burgman, R., 2006. Coseismic and postseismic slip of the 2004 Parkfield earthquake from space-geodetic data, *Bull. Seism. Soc. Am.,* **96,** 269–282.

Lee, J.C., Angelier, J., Chu, H.T., Hu, J.C. & Jeng, F.S., 2001. Continuous monitoring of an active fault in a plate suture zone: a creepmeter study of the Chihshang fault, eastern Taiwan, *Tectonophysics,* **333,** 219–240.

Lee, J.C., Angelier, J., Chu, H.T., Hu, J.C., Jeng, F.S. & Rau, R.J., 2003. Active fault creep variations at Chihshang, Taiwan, revealed by creep meter monitoring, 1998–2001, *J. geophys. Res.,* **108,** doi:10.1029/2003JB002394.

Lee, J.C., Angelier, J., Chu, H.T., Hu, J.C. & Jeng, F.S., 2005. Monitoring active fault creep as a tool in seismic hazard mitigation. Insights from creepmeter study at Chihshang, Taiwan, *C.R. Geosci.,* **337,** 1200–1207.

Lee, J.C., Chu, H.T., Angelier, J., Hu, J.C., Chen, H.Y. & Yu, S.B., 2006. Quantitative analysis of surface coseismic faulting and postseismic creep accompanying the 2003, Mw = 6.5, Chengkung earthquake in eastern Taiwan, *J. geophys. Res.,* **111,** doi:10.1029/2005JB003612.

Leonards, G.A., 1962. Engineering properties of soils, in *Foundation Engineering,* pp. 66–240, ed. Leonard, G.A., McGraw-Hill, New York.

Lienkaemper, J.J., Galehouse, J.S. & Simpson, R.W., 2001. Lon-term monitoring of creep rate along the Hayward fault and evidence for a lasting creep response to the 1989 Loma Prieta earthquake, *Geophys. Res. Lett.,* **28,** 2265–2268.

Lin, C.H., 2004. Repeated foreshock sequences in the thrust faulting environment of eastern Taiwan, *Geophys. Res. Lett.,* **31,** L13601, doi:10.1029/2004GL019833.

Liu, L.B., Roeloffs, E.A. & Zheng, X.Y., 1989. Seismically induced water level fluctuations in the Wali Well, Beijing, China, *J. geophys. Res.,* **94,** 9453–9462.

Marone, C.J., 2000. Shaking faults loose, *Nature,* **408,** 533–535.

Marone, C.J., Scholz, C.H. & Bilham, R., 1991. On the mechanics of earthquake afterslip, *J. geophys. Res.,* **96,** 8441–8452.

Miyazaki, S., Segall, P., Fukuda, J. & Kato, T., 2004. Space time distribution of afterslip following the 2003 Tokachi-oki earthquake: implications for variations in fault zone frictional properties, *Geophys. Res. Lett.,* **31,** doi: 10.1029/2003GL019410.

Okada, Y., 1992. Internal deformation due to shear and tensile faults in a half-space, *Bull. seism. Soc. Am.,* **82,** 1018–1040.

Perfettini, H. & Avouac, J.-P., 2004. Posetseismic relaxation driven by brittle creep: a possible mechanism to reconcile geodetic measurements and the decay rate of aftershocks, application to the Chi-Chi earthquake, Taiwan, *J. geophys. Res.,* **109,** doi:10.1029/2003JB002488.

Perfettini, H. & Avouac, J.-P., 2007. Modeling afterslip and aftershocks following the 1992 Landers earthquake, *J. geophys. Res.,* **112,** doi:10.1029/2006JB004399.

Perfettini, H., Avouac, J.-P. & Ruegg, J.C., 2005. Geodetic displacements and aftershocks following the 2001 Mw = 8.4 Peru earthquake: implications for the mechanics of the earthquake cycle along subduction zones, *J. geophys. Res.,* **110,** doi:10.1029/2004JB003522.

Pollitz, F.F., 2005. Transient rheology of the upper mantle beneath central Alaska inferred from the crustal velocity field following the 2002 Denali earthquake, *J. geophys. Res.,* **110,** doi:10.1029/2005JB003672.

Roeloffs, E.A., 2001. Creep rate changes at Parkfield, California 1966–1999: seasonal, precipitation induced, and tectonic, *J. geophys. Res.,* **106,** 16 525–16 547.

Ruina, A.L., 1983. Slip instability and state variable friction laws, *J. geophys. Res.,* **88,** 10 359–10 370.

Scholz, C.H., 2002. *The Mechanics of Earthquakes and Faulting,* 2nd edn, pp. 471, Cambridge Press, New York.

Todd, D.K., 1959. *Ground Water Hydrology,* pp. 336, John Wiley, New York.

Wu, Y.M. *et al*., 2006. Coseismic versus interseismic ground deformations, fault rupture inversion and segmentation revealed by 2003 Mw 6.8 Chengkung earthquake in eastern Taiwan, *Geophys. Res. Lett.,* **33,** L02312, doi:10.1029/2005GL024711.

Yen, H.Y., Yeh, Y.H., Lin, C.H., Yu, G.K. & Tsai, Y.B., 1990. Free-air gravity map of Taiwan and its applications, *Terr. Atmos. Ocean. Sci.,* **1,** 143–155.

Yu, S.B. & Liu, C.C., 1989. Fault creep on the central segment of the Longitudinal Valley fault, Eastern Taiwan, *Proc. Geol. Soc. China,* **32,** 209–231.

Yu, S.B., Chen, H.Y. & Kuo, L.C., 1997. Velocity field of GPS stations in the Taiwan area, *Tectonophysics,* **274,** 41–59.

© 2008 The Authors, *GJI*, **176,** 601–613
Journal compilation © 2008 RAS